Peroxynitrite induces Alzheimer-like tau modifications and accumulation in rat brain and its underlying mechanisms

Yong-Jie Zhang, Ya-Fei Xu, Ying-Hua Liu, Jun Yin, Hong-Lian Li, Qun Wang, and Jian-Zhi Wang*,[1]

Pathophysiology Department, Key Laboratory of Neurological Disease of Hubei Province, Tongji Medical College, Huazhong University of Science and Technology, Wuhan, P. R. China

ABSTRACT **To investigate the upstream effector that led to tau hyperphosphorylation, nitration, and accumulation as seen in Alzheimer's disease brain, and the underlying mechanisms, we bilaterally injected SIN-1, a recognized peroxynitrite donor, into the hippocampus of rat brain. We observed that the level of nitrated and hyperphosphorylated tau was markedly increased in rat hippocampus 24 h after drug administration, and these alterations were prevented by preinjection of uric acid, a natural scavenger of peroxynitrite. Concomitantly, we detected a significant activation in glycogen synthase kinase-3β (GSK-3β) and p38 MAPKs, including p38α, p38β, and p38δ, but no obvious change was measured in the activity of p38γ, ERK, and c-Jun amino-terminal kinase (JNK). Both nitrated tau and hyperphosphorylated tau were aggregated in the hippocampus, in which the activity of 20S proteasome was significantly arrested in SIN-1-injected rats. Further studies demonstrated that the hyperphosphorylated tau was degraded as efficiently as normal tau by 20S proteasome, but the nitrated tau with an unorderly secondary structure became more resistant to the proteolysis. These results provide the first *in vivo* evidence showing that peroxynitrite simultaneously induces tau hyperphosphorylation, nitration, and accumulation, and that activation of GSK-3β, p38α, p38β, p38δ isoforms and the inhibition of proteasome activity are respectively responsible for the peroxynitrite-induced tau hyperphosphorylation and accumulation. Our findings reveal a common upstream stimulator and a potential therapeutic target for Alzheimer-like neurodegeneration.—Zhang, Y-J., Xu, Y-F., Liu, Y-H., Yin, J., Li, H-L., Wang, Q., Wang, J-Z. Peroxynitrite induces Alzheimer-like tau modifications and accumulation in rat brain and its underlying mechanisms. *FASEB J.* 20, 1431–1442 (2006)**

Key Words: tau · glycogen synthase kinase-3β · p38 MAPKs · proteasome

Neurofibrillary tangle is a defining pathological alteration seen in the brain of Alzheimer's disease (AD). Studies have demonstrated that neurofibrillary tangle is made up of paired helical filament (PHF)/straight filament (SF), and the major protein component of PHF/SF is the hyperphosphorylated microtubule-associated protein tau (1–3). The normal function of tau is to promote microtubule assembly and to stabilize microtubules. When tau is abnormally hyperphosphorylated, as seen in AD brain, it becomes incompetent in binding to and stabilizing microtubules, leading to aberrant aggregation in the neurons. In addition, it has been demonstrated recently that PHF-tau is also nitrated and the nitrated tau is colocalized with neurofibrillary tangle in AD brain (4). Moreover, the nitrated tau also shows a significantly decreased binding activity to microtubules and aggregates in the brains of patients with tauopathies and in peroxynitrite-treated cells (4, 5). These studies together suggest that tau nitration is involved in the formation of filamentous tau inclusions. Hence, not only tau hyperphosphorylation, but also tau nitration appears to contribute to AD pathology. However, the upstream factor(s) leading to both hyperphosphorylation and nitration of tau is not understood.

The majority of cases of sporadic AD are aging dependent. With brain aging, accumulation of oxidants may play an important role in initiating the abnormal posttranslational modifications of tau. For instance, peroxynitrite, the product of the diffusion-limited reaction between NO and superoxide ($k \sim 10^{10}\ M^{-1}s^{-1}$) (6), is a potent nitration mediator and strong oxidant implicated in AD pathogenesis (7–12). Peroxynitrite modifies tyrosine residues in protein and thus generates a stable compound, namely 3-nitrotyrosine (3-NT). As nitration is a permanent footprint, detection of 3-NT is an indicator for peroxynitrite involvement. In AD brain, the concentration of 3-NT was elevated markedly, especially in the hippocampus (7). And the significantly elevated 3-NT was positively correlated with

[1] Correspondence: Department of Pathophysiology, Key Laboratory of Neurological Disease of Hubei Province, Tongji Medical College, Huazhong University of Science and Technology, Wuhan 430030, P.R. China. E-mail: wangjz@mails.tjmu.edu.cn

doi: 10.1096/fj.05-5223com

decreased cognitive functions in AD patients (8). Moreover, uric acid, a proposed endogenous peroxynitrite scavenger, was decreased in a manner consistent with the increases of 3-NT (7), whereas the protein nitration, including tau, increased significantly in AD brain (4, 9–12). These findings strongly suggest that the elevated peroxynitrite may be responsible for the nitration of tau seen in AD.

Does peroxynitrite also contribute to tau hyperphosphorylation? Studies have demonstrated that peroxynitrite, acting as a signaling molecule, regulates mitogen-activated protein kinases (MAPKs) and phosphatidylinositol 3-kinase (PI 3K) -mediated signal transduction pathways. MAPK is a family of serine/threonine kinases activated by dual phosphorylation of tyrosine and threonine residues. They are subdivided into extracellular signal-regulated kinase (ERK), c-Jun amino-terminal protein kinase (JNK), and p38 MAPKs. It was reported that peroxynitrite activated all three MAPKs in a wide variety of cell types (13–19). In contrast to activating MAPKs, peroxynitrite inhibited the PI 3K pathway (20). Peroxynitrite induced nitration of p85 regulatory subunit of PI 3K *in vitro* (21), and this nitration abrogated its interaction with the catalytic subunit p110, thus inhibiting PI 3K activity (22). PI 3K is known to stimulate Akt/PKB, which in turn inhibited the activity of glycogen synthase kinase-3β (GSK-3β) by phosphorylating GSK-3β at Ser-9 (23). Therefore, down-regulation of the PI 3K pathway could lead to overactivation of GSK-3β (22). MAPKs and GSK-3β are proline-directed protein kinases and play important roles in hyperphosphorylation of tau in AD brain (24). From these studies it is suggested that peroxynitrite may induce tau hyperphosphorylation through overactivating MAPKs and GSK-3β.

In the present study we injected bilaterally 3-morpholino-sydnonimine (SIN-1), a recognized and widely used peroxynitrite donor (25–30), into rat hippocampus, and investigated whether or not peroxynitrite could induce simultaneously nitration and hyperphosphorylation of tau and the underlying mechanisms *in vivo*. We found that peroxynitrite could induce nitration/hyperphosphorylation and accumulation of tau. The activation of GSK-3β and the p38 MAPKs family and the inhibition of proteasome proteinase activities are respectively responsible for peroxynitrite-induced tau hyperphosphorylation and accumulation. These findings provide new clues in understanding the role of oxidative and nitrative lesions in AD pathology.

MATERIALS AND METHODS

Materials

Peroxynitrite, SIN-1, and 3-nitrotyrosine monoclonal antibody (mAb) were purchased from Cayman Chemical Co. (Ann Arbor, MI, USA). mAb n847 to nitrated tau, polyclonal antibody (pAb) R134d to total tau, and mAb PHF-1 to PHF-tau phosphorylated at Ser-396/404 were gifts respectively from Dr. John Q. Trojanowski (Center for Neurodegenerative Disease Research, Hospital of The University of Pennsylvania, Philadelphia, PA, USA), Dr. I. Grundke-Iqbal (New York State Institute for basic research, Staten Island, NY, USA), and Dr. P. Davies (Albert Einstein College of Medicine, Bronx, NY, USA). The specificity of n847 for nitrated tau has been characterized (4). Antiphospho-p38 was from R&D Systems, Inc. (Minneapolis, MN, USA). pAb anticleaved caspase-3, antiphospho-ERK, antitotal ERK, antitotal GSK-3β, and antiphospho-GSK-3β at Ser-9 were from Cell Signaling technology, Inc. (Beverly, MA, USA). pAb antiphospho-JNK1&2 and antiphospho-Thr-231 of tau were from BioSource International, Inc. (Camarillo, CA, USA). mAb Tau-1 against tau unphosphorylated at Ser-199/202 was from Chemicon International Inc. (Temecula CA, USA). pAb anti-p85 and the specific GSK-3 substrate phospho-GS peptide were from Upstate Biotechnology Inc. (Lake Placid, NY, USA). Oregon Green 488-conjugated goat anti-mouse IgG (H+L) and rhodamine Red-X-conjugated goat anti-rabbit IgG (H+L) were from Molecular Probes (Eugene, OR, USA). Peroxidase-conjugated goat anti-rabbit and anti-mouse IgG, protein G agarose, phosphocellulose units, and bicinchoninic acid (BCA) protein assay kit were from Pierce Chemical Company (Rockford, IL, USA). Chemiluminescent Substrate Kit and pAb anti-p38 were from Santa Cruz Biotechnology, Inc. (Santa Cruz, CA, USA). 20S proteasome was from Biomol International, LP (Plymouth Meeting, PA, USA). Hoechst 33258, dithiotreitol (DTT), HEPES, ATP, and mAb DM1A to α-tubulin were from Sigma (St. Louis, MO, USA). P11 cellulose phosphate was from Whatman Inc. (Clifton, NJ, USA), Sephacryl S-300 was from Pharmacia Biotech (Uppsala, Sweden). GSK-3β, lactacystin, uric acid, and fluorogenic substrates H-Ala-Ala-Phe-AMC were from CalBiochem (Darmstadt, Germany). γ-^{32}P-ATP was obtained from Beijing Yahui Biological and Medicinal Engineering Co. (Beijing, People's Republic of China).

Hippocampus injection

Male Wistar rats (250±20 g) were obtained from the Experiment Animal Center of Tongji Medical College, Huazhong University of Science and Technology. The rats were trained by Morris water maze (31). Then these rats (n=10 for each group) were deeply anesthetized intraperitoneally with chloral hydrate (30 mg/kg) and placed in a stereotactic instrument. After a skin incision and exposure of the occipital bone, holes were drilled at coordinates of 4.0 mM anterior to posterior (AP) bregma, 2.0 mM mid to lateral (ML), 4.0 mM dorsal to ventral (DV). Rats were injected first into the right hippocampus of 3 μl SIN-1 at 10, 25, and 50 mM, respectively, or 3 μl phosphate-buffered saline (PBS) as vehicle control. A second injection was given at the same coordinates into the left hippocampus. To confirm the effects of peroxynitrite, we infused uric acid (15 μl, 5 mM), a natural scavenger of peroxynitrite (65–68), into the left ventricle of the rats at the coordinates of AP-0.8 mM, ML-1.5 mM and DV-3.8 mM 1 h before the hippocampal injection of SIN-1 (25 mM). All surgical procedures were completed under sterile conditions and penicillin (200,000 U, intramuscularly) was injected to prevent infection. The animals were tested again for spatial memory retention in the water maze 24 h after the drug injection. Though no significant spatial memory deficits were detected in SIN-1-injected rats (data not shown), we found that the training process was crucial for obtaining the reproducible results in tau hyperphosphorylation and GSK-3 activation.

Western blot

Rats were sacrificed 24 h after the injection, and the hippocampus was immediately homogenized at 4°C using a

Teflon™ glass homogenizer in 50 mM Tris-HCl, pH 7.4, 150 mM NaCl, 10 mM NaF, 1 mM Na_3VO_4, 5 mM EDTA, 2 mM benzamidine, 1.0 mM phenylmethylsulfonyl fluoride, 10 μg/ml leupeptin, 10 μg/ml aprotinin, and 10 μg/ml pepstatin. The tissue homogenate was added to one-third volume of sample buffer containing 200 mM Tris-HCl, pH 7.6, 8% SDS, 40% glycerol, 40 mM DTT and boiled for 10 min in a water bath, then centrifuged at 12,000 *g* for 15 min at 25°C. The supernatant was stored at −80°C for Western blot analysis. The protein concentration in the supernatant was measured by BCA kit according to manufacturer's instruction. Equal amounts of protein were separated by a 10% SDS-polyacrylamide gel, then transferred electrically onto nitrocellulose membranes. The membranes were blocked with 5% defatted milk dissolved in TBS-Tween-20 (TBS-T) (50 mM Tris-HCl, pH 7.6, 150 mM NaCl, 0.2% Tween-20) for 1 h at 37°C. The blot was then incubated with mAb n847 (1:500), mAb DM1A (1:1000), pAb R134d (1:5000), mAb PHF-1 (1:500), pAb pThr-231 (1:500), pAb p38 (1:500), pAb phospho-p38 (1:500), pAb ERK (1:500), pAb phospho-ERK (1:500), pAb GSK-3β (1:1000), pAb phospho-GSK-3β (Ser-9 (1:1000), or pAb phospho-JNK1&2 (1:500) overnight at 4°C. The membrane was washed three times with TBS-T, then incubated with anti-mouse or anti-rabbit IgG conjugated to horseradish peroxidase (1:5000) for 1 h at 37°C. The blot was washed three times with TBS-T, then visualized using the enhanced chemiluminescence method. The protein bands were quantitatively analyzed by Kodak Digital Science 1D software (Eastman Kodak Company, New Haven, CT, USA). The level of total tau was calculated based on α-tubulin, and the level of nitrated tau and hyperphosphorylated tau was normalized by total tau; all tau bands, which may result from differential posttranslational modifications and degradation commonly seen in tau proteins, have been quantitatively analyzed as a one band per lane. The level of phospho-p38 MAPKs, phospho-ERK, phospho-GSK-3β, and nitrated p85 was normalized by total p38, ERK, GSK-3β, and p85, respectively. All were expressed as relative level of the sum optical density against corresponding control.

GSK-3 activity assay

The hippocampus was homogenized as described above and the homogenate was centrifuged at 12,000 *g* for 20 min at 4°C. The resulting supernatant was assayed for GSK-3 activity using phospho-GS peptide 2 as described previously (47,63). Briefly, 7.5 μg protein was incubated for 30 min at 30°C with 20 μM peptide substrate and 200 μM γ-^{32}P ATP (1,500 cpm/pmol ATP) in 30 mM Tris, pH7.4, 10 mM $MgCl_2$, 10 mM NaF, 1 mM Na_3VO_4, 2 mM EGTA, and 10 mM β-mercaptoethanol in a total volume of 25 μl. The reaction was stopped with 25 μl of 300 mM *o*-phosphoric acid. Then 25 μl of the reaction mixture was applied in duplicates to phosphocellulose units. The filters were washed 3 times with 75 mM *o*-phosphoric acid, dried and analyzed by a liquid scintillation counter (1450 MicroBeta JET, PerkinElmer Life and Analytical Sciences, Shelton, CT, USA). Relative activity of GSK-3 activity was expressed.

Immunoprecipitation

As the most obvious changes in GSK-3β and tau modifications were observed at 25 mM of SIN-1 administration, we used this concentration for the mechanism studies. Rats were sacrificed 24 h after the injection with 25 mM SIN-1. The hippocampus was quickly dissected out and homogenized in 9 volumes (m/v) of ice-cold modified radio-immunoprecipitation assay buffer (50 mM Tris-HCl, pH 7.4, 150 mM NaCl, 1% Nonidet P-40, 0.25% Na-deoxycholate, 1 mM EDTA, 1 mM PMSF, 1 μg/ml each aprotinin, leupeptin, and pepstatin, 1 mM Na_3VO_4, 1 mM NaF). After spinning the homogenate at 14,000 *g* for 15 min at 4°C, the supernatant (1 ml) was incubated with 100 μl of protein G agarose on a shaker for 10 min at 4°C to remove the nonspecific binding protein. The protein G beads were removed by spin at 14,000 *g* for 10 min at 4°C. The supernatant (750 μg protein in 1 mg/ml) was incubated with 4 μg of anti-p85 antibody (Ab) overnight at 4°C with gentle shaking. The Ag/antibody immunocomplex was captured by further incubating with 100 μl of PBS-washed protein G agarose beads for 2 h and spinning for 5 s at 14,000 *g*. The beads were washed three times with PBS and resuspended in 60 μl 2 × sample buffer. After boiling for 5 min in water bath, the supernatant was collected by centrifugation at 14,000 *g* for 1 min. Finally, the proteins were analyzed by Western blot with pAb p85, and the same membrane was stripped and reprobed with mAb 3-nitrotyrosine to detect the nitrated p85.

Immunofluorescence

Rats were anesthetized and transcardially perfused with 200 ml normal saline (NS), then perfused with 400 ml 4% paraformaldehyde solution 24 h after injection of 25 mM SIN-1 or vehicle. The brain was removed from the skull and postfixed in the same solution for 12 h at 4°C, then sliced into 30 μm coronary sections with a Vibratome (LANCER, S100, TPI, Germany). For confocal image analysis, the 30 μm vibratome sections were permeabilized with 0.5% Triton X-100-PBS for 30 min. The sections were blocked with 5% BSA for 1 h at 37°C and incubated with either mAb n847 (1:500), or mAb PHF-1 (1:250), or pAb cleaved caspase-3 (1:100) for 48 h at 4°C, followed by 1 h at room temperature. After washing with PBS, sections were incubated with Oregon Green 488-conjugated goat anti-mouse IgG (H+L) (1:1000) (n847 and PHF-1) or rhodamine Red-X-conjugated goat anti-rabbit IgG (H+L) (1:1000) (cleaved caspase-3) for 2 h at 37°C in the dark, then Hoechst 33258 (10 μg/ml) was added to stain the nuclei. Sections were washed and mounted in PBS with 10% glycerol, and fluorescence was measured using Olympus FV500 Laser Scanning Confocal microscope (Olympus Optical, Tokyo, Japan).

Quantitative analysis of the cell nuclei and activated caspase-3-positive cells

The cell viability in the hippocampus of the SIN-1- or PBS-(control) injected rats was measured by counting the number of cells labeled with Hoechst 33258. The cell apoptosis was estimated by immunostaining of the cells with the activated form of caspase-3 Ab. Six sections at a 90 μm interval in each rat (3 rats for each group) were used for quantitative analysis by using Image-Pro Plus 4.5 system (Media Cybernetics, Inc., Silver Spring, MD, USA). The number of the cells was counted in six fields of each section at an original magnification of ×200 by using Olympus FV500 Laser Scanning Confocal Microscope (Olympus Optical, Tokyo, Japan).

Measurement of proteasome activity

Proteasome activity was determined by assaying the chymotrypsin-hydrolase peptide hydrolyzing activity (32,33). Briefly, 250 μl hippocampus homogenate (2 μg/μl), prepared with 10 mM Tris-HCl, pH 7.2, 0.035% SDS, 5 mM $MgCl_2$, and 5 mM ATP, were incubated with 5 mM (2.5 μl) synthetic substrate (H-Ala-Ala-Phe-AMC) at 37°C for 1 h, then the released concentration of 7-amido-4-methylcoumarin (AMC)

was measured by fluorimetry at 370 nM excitation and 430 nM emission using Molecular Devices SPECTRAmax M2 Fluorescent Microplate Reader (Process Analysis and Automation Ltd, Hampshire, UK). The activity of proteasome was expressed by subtracting the background value, which was determined by incubating the reaction mixture with 50 μM of lactacystin, a proteasome inhibitor, for 30 min before the addition of proteasome substrate.

Purification, nitration, and phosphorylation of tau *in vitro*

Human tau 39 (Htau39) was expressed in *E. coli* strain BL21. The recombinant tau protein was isolated and purified by phosphocellulose chromatography followed by Sephacryl S-300 Gel filtration (5). The nitration of tau by peroxynitrite was carried out as described previously (5). Briefly, Htau39 (1 mg/ml) dissolved in reaction buffer (100 mM potassium phosphate, 25 mM sodium bicarbonate, and 0.1 mM diethylenetriamine pentaacetic acid, pH 6.4) was reacted with decomposed peroxynitrite or 1 mM authentic peroxynitrite at 37°C for 10 min with robust shaking. The concentration of stock peroxynitrite was determined by measuring the absorbance at 302 nM (ε_{302}=1670 $M^{-1}cm^{-1}$). After reaction, the nitration of tau was determined by Western blot with mAb 3-nitrotyrosine. Phosphorylation of tau by GSK-3β was carried according to the method described (34). Briefly, Htau39 was incubated in the absence or presence of GSK-3β (50 munits/ml) in a reaction mixture containing 0.25 mg/ml of tau, 10 mM $MgCl_2$, 5 mM DTT, 2 mM ATP, 20 mM HEPES, pH 7.5. The reaction was initiated by the addition of the kinase. After incubation at 30°C for 4 h, the reaction was stopped by heating at 95°C for 10 min and the denatured kinase was removed by centrifugation (10,000 *g* for 10 min). The phosphorylation of tau was determined by Western blot with PHF-1 Ab.

In vitro degradation of tau with 20S proteasome

The degradation of tau by 20S proteasome *in vitro* was measured by a method described previously (35). Briefly, recombinant normal tau, phosphorylated tau, and nitrated tau were diluted to a final concentration of 200 nM and incubated with or without 10 nM purified human erythrocyte 20S proteasome in 30 μl reaction mixture containing 50 mM Tris-HCl, pH 7.5, 0.02% Tween-20 (v/v). The mixture was incubated at 37°C for 1 h or 4 h and the reaction was terminated by addition of one-third volume of sample buffer. Tau degradation was revealed by Western blot with pAb R134d as described above.

Circular dichroism spectroscopy

Circular dichroism (CD) spectra from normal tau or nitrated tau (0.1 mg/ml) in water were taken using Jasco J-810 spectrapolarimeter (Jasco international Co. Ltd, Tokyo, Japan). The CD spectra were recorded in the range of 190–250 nM using a 0.1 cm path length quartz cuvette at 25°C in continuous scanning mode. The acquisition parameters were 100 nM/min, with a 1.0 s response and a 1.0 nM band width. The data were accumulated over 10 runs, the presented data being the average. The results were expressed in term of molecular ellipticity [θ] in unit of $deg.cm^2/dmol$.

Statistical analysis

Data were analyzed using statistical Packages for the Social Sciences 10.0 statistical software. The 1-way ANOVA procedure followed by least significant differences post hoc tests was used to determine the statistical significance of differences of the means.

RESULTS

Effects of SIN-1 in nitration and hyperphosphorylation of tau and cell viability in rat hippocampus

After injection of 10, 25, and 50 mM of 3.0 μl SIN-1 into the hippocampi of the rat brains, we found an increase of tau nitration to 2.2- ($P<0.01$), 2.7- ($P<0.01$), and 2.7-fold ($P<0.01$), respectively, of the control level as measured by Western blots developed with Ab n847 (**Fig. 1*A, B***). This increase of tau nitration confirms the production of peroxynitrite in the injected rat hippocampus; then changes in the phosphorylation concentration of tau were examined by using phosphorylation-dependent and site-specific tau antibodies. We found that the level of phosphorylated tau (at PHF-1 epitope) increased to 1.5- ($P<0.01$), 1.5- ($P<0.01$), and 1.3-fold ($P<0.05$) of the control concentration in SIN-1-injected rats (Fig. 1*A, B*). The phosphorylation concentration of tau at Thr231 was also significantly increased, but no change was seen at tau-1 sites (not shown). The level of nitrated and phosphorylated tau was normalized by total level of tau, the latter was also increased to 1.1-, 1.2-, and 1.1-fold of the control levels at 24 h after injection of SIN-1 (Fig. 1*A, B*). To further confirm the role of peroxynitrite, we injected uric acid, a natural scavenger of peroxynitrite (65–68), into the rat before injection of SIN-1. We observed that preadministration of uric acid prevented tau from nitration and hyperphosphorylation (Fig. 1*C, D*). We also observed that the hyperphosphorylation and nitration of tau was no longer obvious at 48 h after the injection of SIN-1 (not shown). These results together demonstrated that peroxynitrite, produced by SIN-1, can induce in rat brain both tau nitration and hyperphosphorylation within 24 h after administration of the drug. The increased total tau suggests accumulation of nitrated and hyperphosphorylated tau.

To determine the effect of SIN-1 injection on cell viability, we measured the cell loss by counting the nuclei of the cells stained with Hoechst 33258. It was shown that the average number of nuclei in the hippocampus was not significantly changed ($P>0.05$) after the injection of SIN-1 (Fig. 1*E*). To further assess the cell apoptosis, we stained the cells with the activated caspase-3 Ab. Almost no positive staining was detected in the hippocampus of the SIN-1- (Fig. 1*E*, left panel) and PBS- (not shown) injected rats. As negative results for the activated caspase-3 were seen in both SIN-1 and PBS-injected rats, we injected staurosporine (0.5 mM, 3 μl), a recognized apoptotic inducer activating caspase-3 (70), into the rats to serve as a positive control. Many neurons with activated caspase-3 were seen in the staurosporine-injected hippocampus (Fig. 1*F*, right panel). These results indicate that the single injection of SIN-1 does not induce significant cell loss and cell apoptosis.

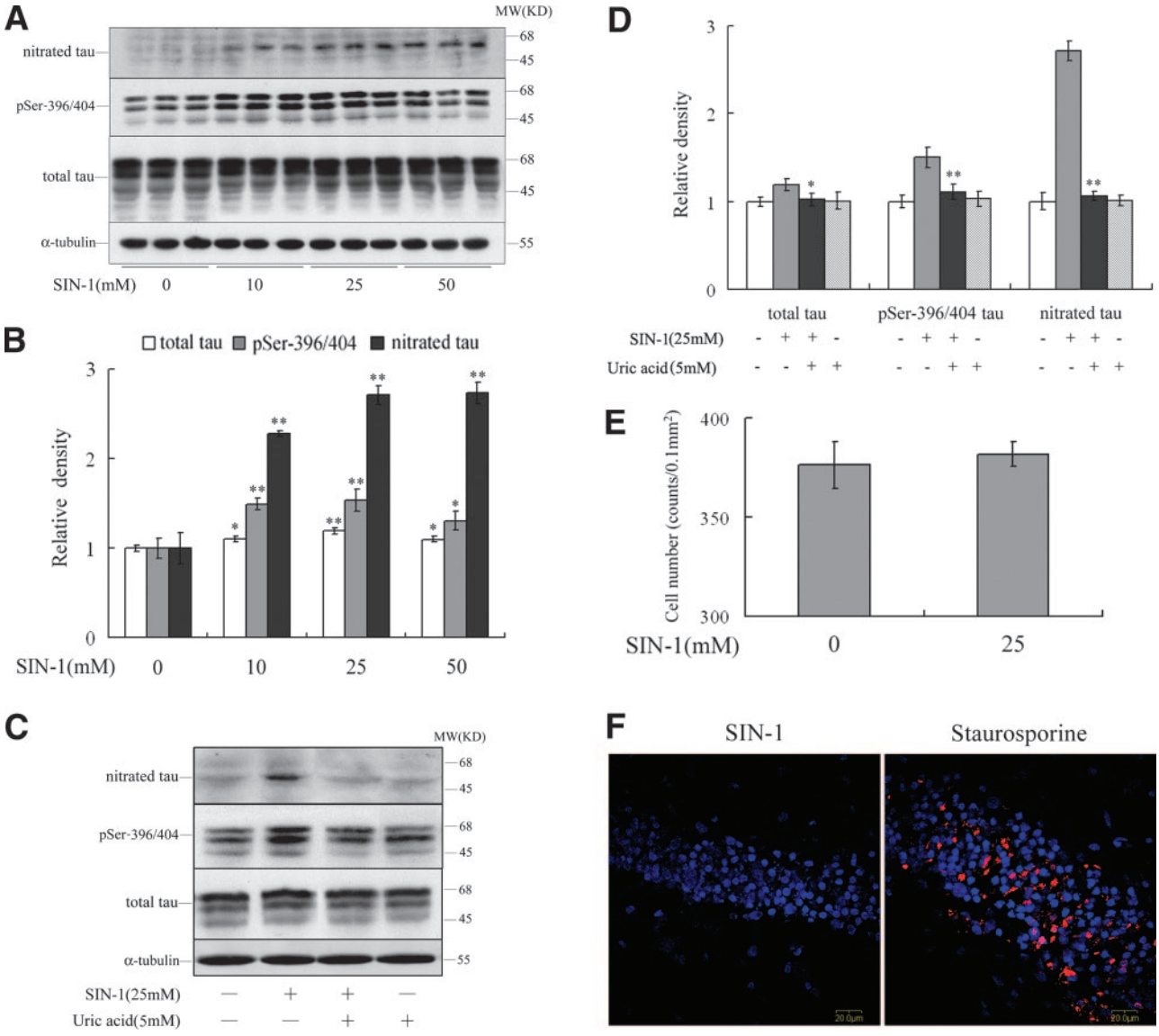

Figure 1. Effects of SIN-1 on nitration and hyperphosphorylation of tau and cell viability in rat hippocampus. Western blot (*A*) and quantitative analysis (*B*) data demonstrated that the levels of nitrated and hyperphosphorylated tau (normalized by total tau) as well as total tau (normalized by α-tubulin) were elevated 24 h after injection of SIN-1. Uric acid prevents efficiently tau proteins from SIN-1-induced nitration and hyperphosphorylation (*C, D*). No obvious cells lost or cell apoptosis was observed. The cell loss was measured by counting the numbers of the cell nuclei stained with Hoechst 33258 (*E*). The cell apoptosis (F) was assessed by double-staining confocal microscopy with Hoechst 33258 (blue) and cleaved caspase-3 (red). The positive control (*F*, right panel) treated with staurosporine was used to ensure the validity of the staining system. The results were expressed as the mean ± SE. (n=3) (*B, E*), mean ± SD (n=3) (*D*). *$P < 0.05$, **$P < 0.01$ *vs.* controls. Scale bar = 20 μm (*F*).

Protein kinases involved in tau hyperphosphorylation in SIN-1-injected rats

To understand the underlying mechanisms for peroxynitrite-induced tau hyperphosphorylation, we measured the activities of GSK-3β and MAPKs because peroxynitrite has been shown to activate both kinases *in vitro*, and both kinases efficiently phosphorylate tau at Ser-396/404 sites. We found that although the concentration of total GSK-3 was not changed, the concentration of Ser-9-phosphorylated GSK-3β (inactivated form) was decreased to 44% (P<0.01), 39% (P<0.01), and 41% (P<0.01) of the control levels after injection of the rats with 10, 25 and 50 mM of SIN-1, respectively (**Fig. 2*A, B***). The activation of GSK-3 in the SIN-1-injected rats was further confirmed by ^{32}P-labeling assay of the enzyme activity. The results showed that the activity of GSK-3 in rat hippocampus was increased to 2.1- (P<0.01), 2.5- (P<0.01), and 2.2-fold (P<0.01) of the control levels (Fig. 2*C*) in response to the treatment with 10, 25, and 50 mM SIN-1, respectively. It is also reported that p85 is a target for peroxynitrite-induced protein nitration, and this nitration may consequently activate GSK-3β via inhibiting PI 3K-mediated pathway (22). To test this, we measured the nitration of p85 by immunoprecipitation and detected a significantly increased level of nitrated p85 protein in SIN-1-injected rats (Fig. 2*D, E*) (P<0.01). These results suggest that

activation of GSK-3β may be involved in peroxynitrite-induced tau hyperphosphorylation, and simultaneous nitration of p85 may be an upstream regulator for the activation of GSK-3β.

Then the involvement of MAPKs family was measured by using activity-dependent antibodies (represented by phosphorylation). It was shown that the concentration of phosphorylated p38 isoforms, i.e., p38α, p38β, p38δ but not p38γ was significantly increased in SIN-injected rats (Fig. 2*F, G*). No remarkable alteration was observed in ERK and JNK and the concentration of phosphorylated-ERK was even de-

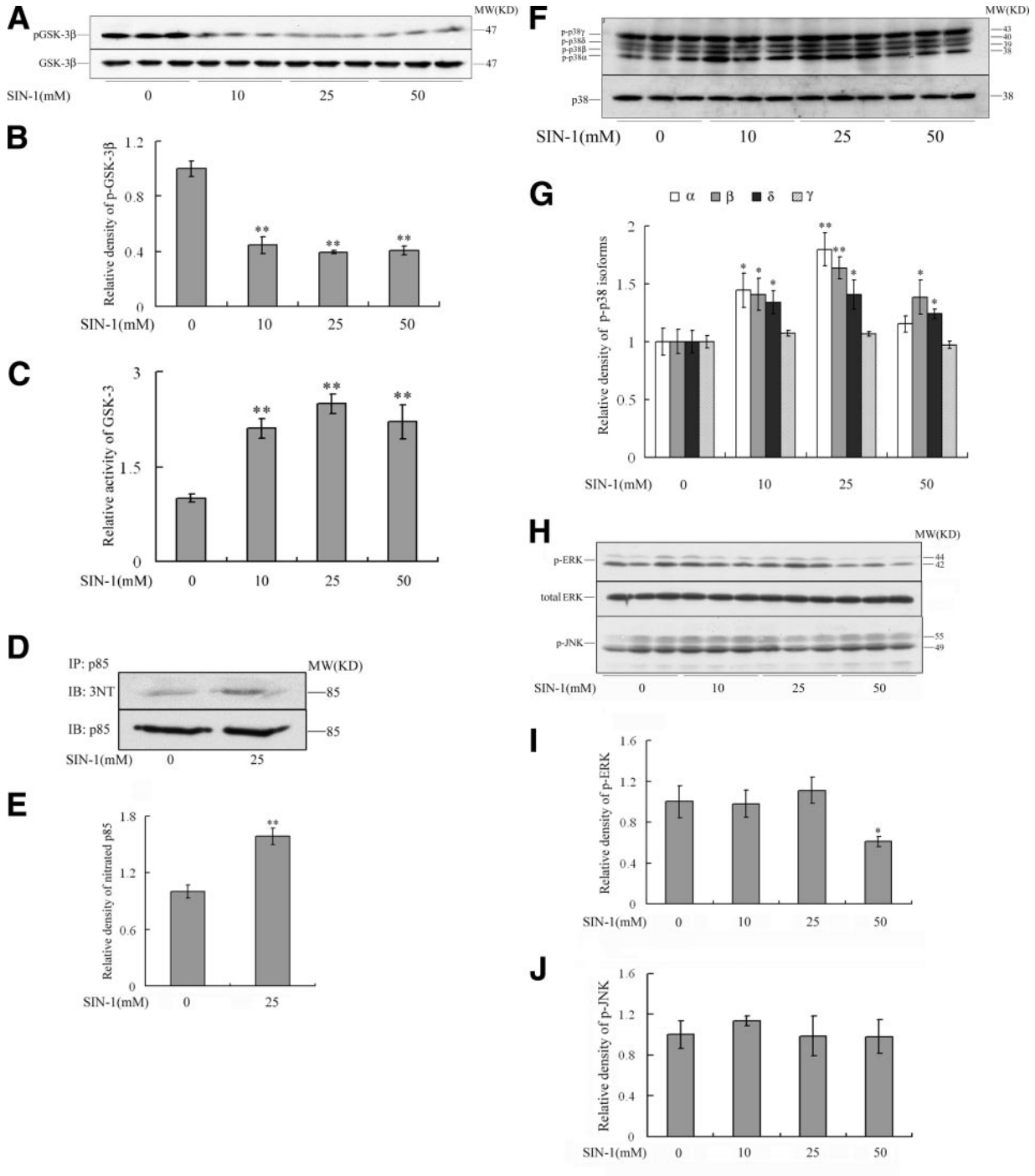

Figure 2. Activation of GSK-3β and p38 MAPKs in SIN-injected rats. Western blot (*A, D, F, H*) and the quantitative analysis (*B, C, E, G, I, J*) were shown. Activation of GSK-3 in SIN-1-injected rats was observed by decreased ratio of Ser-9-phosphorylated GSK-3β to the total concentration of the enzyme (*A, B*) and by ^{32}P-labeling assay of the enzyme activity (*C*). The concentration of the nitrated p85 prepared by immunoprecipitation was elevated (*D, E*), and levels of the activated p38 MAPKs, including p38α, p38β, and p38δ, were also increased in SIN-1-treated rats (*F, G*), but levels of p38γ (*F, G*), ERK (*H, I*), and JNK (*H, J*) were not changed obviously at the same condition. The results were expressed as the mean ± SE. (n=3) (*B, G, I, J*), mean ± SD (n=3) (*C, E*). *$P < 0.05$, **$P < 0.01$ *vs.* controls.

creased significantly at 50 mM of SIN-1 group (Fig. 2*H–J*). These data suggest that peroxynitrite may only selectively activate p38α, p38β and p38δ but not p38γ, ERK and JNK. And the activation of p38α, p38β and p38δ may contribute to the peroxynitrite-induced tau phosphorylation in these rats.

Accumulation of nitrated and hyperphosphorylated tau in SIN-1-injected rat hippocampus

To investigate the cellular distribution of both nitrated and phosphorylated tau in the hippocampus of the rats, we did immunofluorescence staining and analysis by confocal microscopy. We observed that in addition to a significantly enhanced immunoreaction of nitrated tau in CA2 (**Fig. 3*A***), CA3 (Fig. 3*B*) and CA4 (Fig. 3*C*) regions of the hippocampus, two types of staining profile were observed in SIN-1-injected rats. First, the nitrated tau was evenly stained in the cytoplasmic compartment, and this type of staining profile accounted for the majority of neurons both in SIN-1-treated (yellow arrow, Fig. 3) and vehicle-treated control samples, although the latter showed much weaker staining (Fig. 3). Second, the nitrated tau was largely accumulated in the perikarya and dendrites (white arrow and Fig. 3*D*), as seen in AD brain (4); this type of staining profile was seen exclusively in cells of SIN-1-injected rats.

The staining intensity for the phosphorylated tau at PHF-1 epitope in SIN-1-treated rats was markedly increased compared with that of control rats in CA3 and CA4 regions of the hippocampus (**Fig. 4**). In the CA3 sector of the SIN-1-treated rats, the most dramatically increased staining of PHF-1 was largely located in the mossy fibers (Fig. 4*A*); although immunofluorescence was also shown in cell bodies of the pyramidal neurons (yellow arrow, Fig. 4*A*), the latter was not detected in the control slices. In the CA4 sector of the SIN-1-treated rats, the phosphorylated tau at PHF-1 epitope was not only markedly increased in the neurofibers but also aggregated into the cell body and hillock of the cells to form tangle-like morphology (white arrow, Fig. 4*B, C*). The fluorescence with PHF-1 was almost undetected in the CA4 sector of the control rats (Fig. 4*B*). These results together suggested that peroxynitrite could induce not only tau nitration/hyperphosphorylation but also tau accumulation in rat brain.

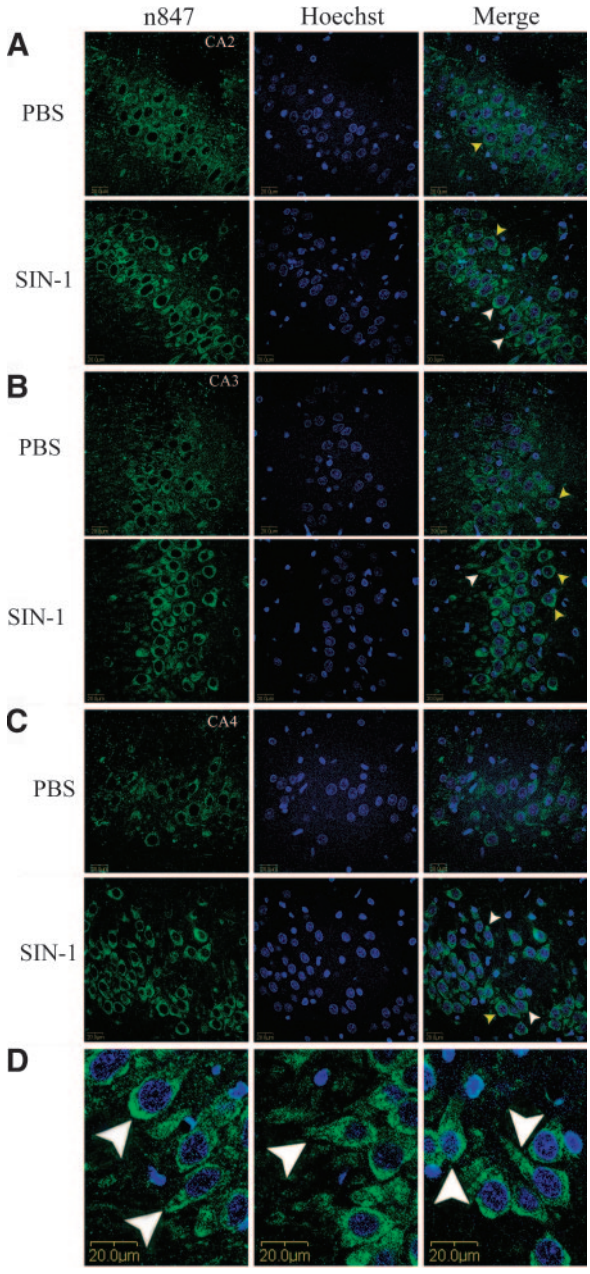

Figure 3. Accumulation of nitrated tau in the hippocampus of the SIN-1-injected rats. Double-staining confocal microscopy with n847 (green) and Hoechst 33258 (blue) were used. The nitrated tau were evenly distributed in the cytoplasmic compartment of the majority SIN-1-treated and control sections (30 μm), but the staining in the control was much weaker (yellow arrow); accumulation of the nitrated tau (white arrow and panel *D*) was seen exclusively in SIN-1-treated rats. Scale bar = 20 μm.

The involvement of proteasome in tau accumulation in SIN-1-injected rat hippocampus

To explore the underlying mechanism for peroxynitrite-induced tau accumulation, we measured the activity of proteasome in rats treated with 25 mM SIN-1. We found that the proteasome activity was decreased to 39% of control levels after SIN-1 injection (**Fig. 5*A***), suggesting the inhibition of proteasome activity by peroxynitrite. Next we analyzed the degradative nature of the phosphorylated and nitrated tau by 20S proteasome *in vitro*. We found unexpectedly that phosphorylated tau at PHF-1 epitope by GSK-3β (Fig. 5*B*) could be degraded as efficiently as normal tau (even better at 4 h) by 20S proteasome (Fig. 5*C, D*). On the other hand, we also observed that ~80% full-length nitrated tau (~62 kDa) was not degraded by 20S proteasome while the unnitrated tau was almost completely degraded at 4 h of the reaction (**Fig. 6*A, B***). To further understand the role of structural elements in the proteolysis-resistant property of the nitrated tau, we

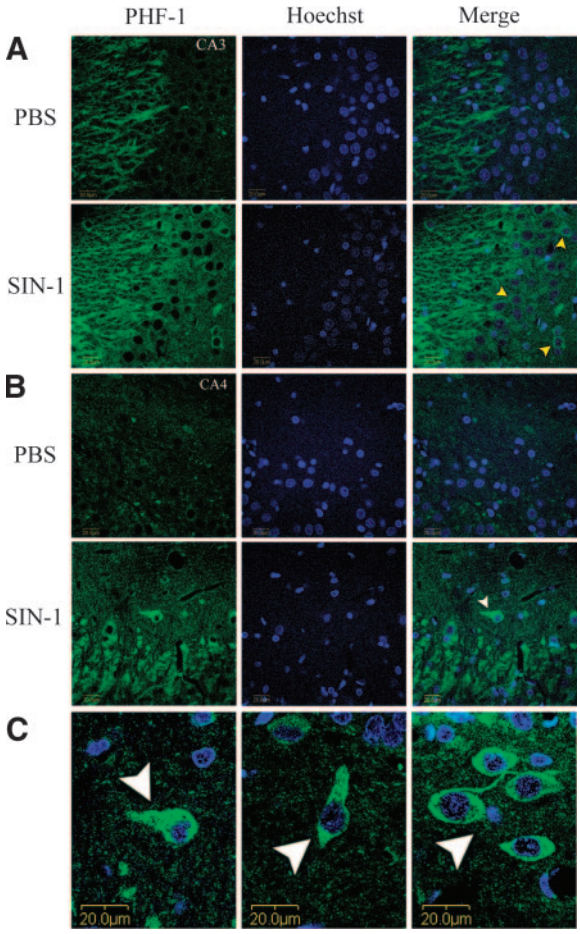

Figure 4. Accumulation of the hyperphosphorylated tau in the hippocampus of the SIN-1-injected rats. Double-staining confocal microscopy with PHF-1 (green) and Hoechst 33258 (blue) was used. Only weak staining of PHF-1 was seen in the mossy fibers of the CA3 sector in control rats, whereas increased staining of PHF-1 was observed in the mossy fibers and the pyramidal neural cells of the SIN-1-injected rats (yellow arrow) (*A*); some tangle-like neurons were seen (white arrow and panel *C*) in the CA4 region (*B*) of the hippocampus of SIN-1-injected rats. Scale bar = 20 μm.

measured the secondary structure of nitrated tau by CD spectra analysis. We observed a strong negative peak at 200 nM wavelength (Fig. 6*C*) representing a more unordered conformation or a significant change of secondary structure in the nitrated tau protein. These data together indicate that peroxynitrite may induce tau accumulation through inhibiting 20S proteasome and accelerating tau nitration.

DISCUSSION

Alzheimer's disease is the most common neurodegenerative disorder. A pathological hallmark lesion seen in AD brain is the intracellular accumulation of the abnormally modified tau protein. In addition to be hyperphosphorylated, tau in AD brain is also nitrated, but the upstream factor(s) leading simultaneously to these modifications of tau is not understood. Increasing evidence suggests that oxidative stress is closely related to nitrative injury in AD patients. For instance, a widespread occurrence of 3-nitrotyrosine, an indicator of peroxynitrite, in neurons of AD patients suggests that peroxynitrite is excessively produced in AD brain. Peroxynitrite is a strong oxidant, and it is formed from NO and superoxide at a high rate. In AD brain, all three isoforms of NO synthases (NOS) are aberrantly expressed in different cell types and the expression of NOS is structurally related to the formation of 3-nitrotyrosine, indicating that excessive production of NO results in the formation of peroxynitrite (36). In addition, Aβ deposited as senile plaque in AD brain can stimulate production of NO and superoxide through activating microglia and astrocytes (37–42). These data together suggest that formation of peroxynitrite from excessive production of NO and superoxide in AD brain may be an upstream effector for both tau hyperphosphorylation and nitration. In the present study we tested this speculation by injecting bilaterally SIN-1, a widely recognized and commonly used peroxynitrite-generating compound (25–30), into rat hippocampus. We found that the levels of both nitrated and hyperphosphorylated tau were markedly increased after the drug administration. These results indicate that per-

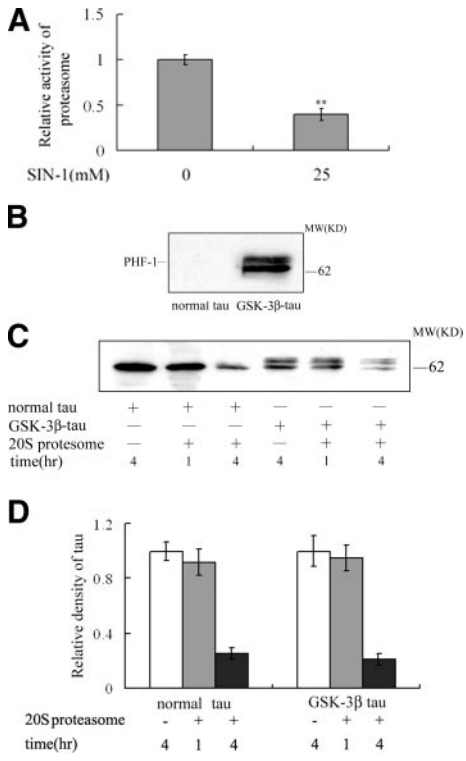

Figure 5. Inhibition of proteasome activity in SIN-1-injected rats and the *in vitro* degradation of hyperphosphorylated tau by the proteasome. The proteasome activity was decreased in the hippocampus of the SIN-1-injected (25 mM) rat (*A*). *In vitro* phosphorylation of tau by GSK-3β was confirmed with PHF-1 (*B*). The GSK-3β-phosphorylated tau was degraded as efficiently as normal tau by the commercially purchased purified 20S proteasome (*D*). Results were expressed as the mean ±SD (n=3); $^{**}P < 0.01$ *vs.* controls.

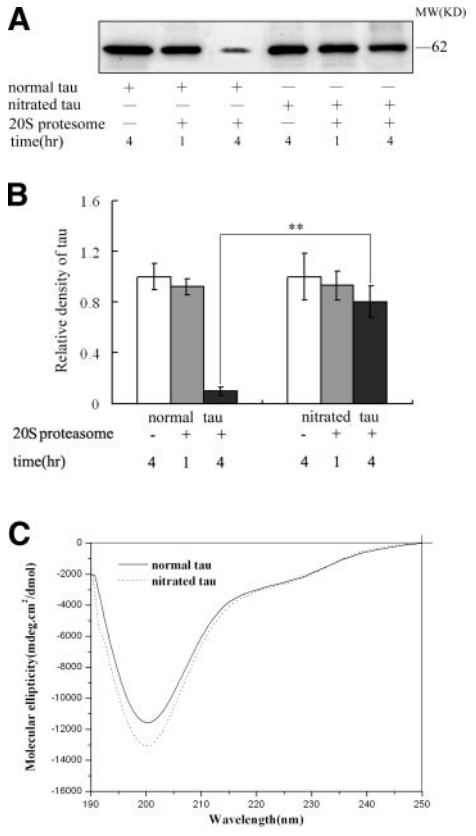

Figure 6. Resistance of the *in vitro* nitrated tau to 20S proteasome. Equal amount of normal tau (treated with decomposed peroxynitrite) and the nitrated tau (treated with authentic peroxynitrite) was incubated with 20S proteasome for 1 h or 4 h, as indicated, and tau degradation was determined by Western blot. Increased resistance of nitrated tau to 20S proteasome (*A, B*) and a strong negative band at 200 nM (*C*) were seen in SIN-1-injected rats. The results were expressed as the mean ± SD (n=3); $^{**}P < 0.01$ *vs.* controls.

oxynitrite, generated from SIN-1, can indeed serve as an *in vivo* mediator for simultaneous nitration and hyperphosphorylation of tau as seen in AD brain. We also observed that the abnormal modifications of tau induced by SIN-1 were no longer obvious 48 h after the injection. This suggests that the Alzheimer-like tau alterations induced by single injection of the drug are reversible. We did not observe any obvious cell death at 24 h after the injection of the drug, suggesting that the acute tau hyperphosphorylation and accumulation might not be toxic to the cells. This is supported by recent studies, which suggest that tau phosphorylation and accumulation may represent a protective function in AD (71, 72). AD is a chronic neurodegenerative disorder, and thus the peroxynitrite-related oxidative stress (7–12) may be a long-drawn event. Therefore, in future study a prolonged infusion of the drug is necessary to disclose the role of chronic oxidative damage in AD development.

To our knowledge, nitration of tau induced by peroxynitrite seems to be simply a chemical reaction (6,43), i.e., the reaction becomes stronger when the protein is subjected to the environment with elevated peroxynitrite. Therefore, we did not pursue the mechanism study for peroxynitrite-induced tau nitration. For the mechanism of tau hyperphosphorylation, we found that the activity of GSK-3β, a crucial kinase involved in Alzheimer-like tau hyperphosphorylation, was significantly increased in SIN-1-injected rats. GSK-3β is abundant in the central nervous system. The active form of GSK-3β accumulates in the cytoplasm of pretangle neurons and its distribution in AD brains is coincident with the sequence of development of neurofibrillary alterations (44, 45). Furthermore, GSK-3β was shown to phosphorylate tau at multiple PHF-tau sites, including PHF-1 and pThr-231 (46), and overactivation of GSK-3β by inhibition of PI 3K led to tau hyperphosphorylation (47, 48). Therefore, activation of GSK-3β may play a key role in the tau hyperphosphorylation observed in SIN-1-injected rats. It is known that the activity of GSK-3 is regulated by the upstream PI3K/PKB and nitration of the regulatory subunit of PI 3K, i.e., p85, down-regulates PI 3K. The level of nitrated p85 was significantly elevated, which may at least partially contribute to the overactivation of GSK-3β in the SIN-1-injected rats.

In addition to GSK-3β, the p38 MAPK family (i.e., α, β, and δ) was also stimulated in SIN-1-injected rats. It was reported that p38 MAPKs could phosphorylate tau in a manner similar to the PHF-tau characterizing AD (49, 50), and the kinases as well as its activator, MKK6, were aberrantly activated in neurons containing filamentous tau in AD brain (51–54). A recently *in vitro* study demonstrated that p38 could phosphorylate tau at Ser-396/404 sites (55). These data suggest the involvement p38α, β, and δ in tau hyperphosphorylation in SIN-1-treated rats. The activities of p38γ, ERK, and JNK were not changed significantly after SIN-1 administration, ruling out the role of these kinases in the system.

We also found in the present study that both hyperphosphorylated and nitrated tau were accumulated in the SIN-1-injected rats. According to the observed morphological characteristics, we presume that the hyperphosphorylated and nitrated tau might be primarily deposited in the neurons. However, the possibility of the glial distribution of the modified tau was not ruled out because the hyperphosphorylated (33) and nitrated tau (4) were also found in the filamentous glial tau inclusions, a prominent brain lesion of the tauopathies (69).

To understand the underlying mechanism for the observed tau aggregation, we designed to analyze tau degradation by 20S proteasome according to the following reasons. First, 20S proteasome is structurally the core and functionally the catalytic subunit of 26S proteasome (73); therefore, interpreting the function of 20S proteasome on tau degradation is significant for understanding the roles of ubiquitin-proteasome system on the turnover of the particular proteins. Second, 20S proteasome presents independently in the cells, and the amount of 20S proteasome is ~ 2.5-fold higher than that of 26S protease (74), indicating the indepen-

dent role and the significance of the 20S proteasome. Third, it has been reported that 20S proteasome can degrade normal tau (35, 64), but the nature of this proteinase on the degradation of the hyperphosphorylated and nitrated tau was unknown. We have demonstrated for the first time that 20S proteasome plays different roles in degradation of hyperphosphorylated and nitrated tau proteins (i.e., it degrades the *in vitro* GSK-3β-phosphorylated tau as efficiently as normal tau) but the nitrated tau resists to the proteolysis by 20S proteasome. We also found that the activity of 20S proteasome was significantly decreased in the hippocampus of the SIN-1-injected rats. This result was in agreement with the previous study in hepatocytes that peroxynitrite directly inhibited the 20S proteasome activity (56). From these data, we speculate that the peroxynitrite-induced accumulation of the hyperphosphorylated tau is relevant to the inhibition of 20S proteasome. A significantly decreased proteasome activity was also observed in AD brain (32, 57, 58). Moreover, it was also reported that tau hyperphosphorylation and aggregation were only transiently expressed in okadaic acid-treated OLN-t40 cells, but hyperphosphorylation followed by proteasome inhibition led to stable deposition of the fibrillary tau (33). Our results *in vivo* further confirm the notion that the decline of proteasome activity contributes to AD pathology, especially in the formation of tau aggregates.

Tau nitration is also implicated in the formation of tau inclusions (4, 5). Although a recent study indicates that nitration inhibits *in vitro* tau polymerization (59), the present study gives direct evidence that nitrated tau aggregates in the hippocampus *in vivo*. Mechanisms leading to the aggregation of nitrated tau may be due to both decreased proteasome activity and increased resistance to the proteolysis; the latter may be relevant to the structural alteration of the nitrated tau. This is supported by a study showing that nitrated α-synuclein is proteolyzed by 20S proteasome at a slower rate than control; nitration also induces a more unorderly secondary structure of α-synuclein (60), which has similar biological and biophysical properties to tau in both normal and pathological states (61). Moreover, proteasome inhibition is also believed to contribute to the aggregation of the nitrated tau, because proteasomal inhibition by lactacystin is associated with an increased protein nitration and the formation of nitrated protein aggregates (62). To understand the relationship between tau hyperphosphorylation and nitration and the proteolytic characteristics of this type of tau to the proteasome, we tried to simultaneously nitrate and phosphorylate tau *in vitro*. But we found unexpectedly that prephosphorylation of tau inhibited its nitration by peroxynitrite and prenitration of tau inhibited its phosphorylation by GSK-3β. The *in vivo* relationship between tau phosphorylation and nitration needs further study.

Taken together, the present study has provided the first *in vivo* evidence showing that peroxynitrite induces nitration, hyperphosphorylation and accumulation of tau. The concurrent activation of GSK-3β and p38 MAPKs may be responsible for the tau hyperphosphorylation while the combined effects of proteasome inhibition and proteasomic resistance (for nitrated tau) may be the underlying mechanisms for tau aggregation. These results provide new insight into the deregulatory pathways in AD pathology. FJ

We thank Dr. C.-X. Gong of the NYS Institute for Basic Research, Staten Island, NY, USA, for critical reading of the paper, and Drs. K. Iqbal and I. Grundke-Iqbal of the same institute for scientific discussion and reagents. We thank Dr. J. Q. Trojanowski of the Center for Neurodegenerative Disease Research, Hospital of The University of Pennsylvania (Philadelphia, PA, USA) for Ab n847 and Dr. P. Davies of the Albert Einstein College of Medicine (Bronx, NY, USA) for Ab PHF-1. We also thank Q. H. Pan of the Chemistry Department of Huazhong University of Science and Technology for technical assistance of Circular Dichroism Spectroscopy. This work was supported in part by grants from the National Natural Science Foundation of China (30500086 and 30430270) and National Major Grant for Basic Research (2006CB500703).

REFERENCES

1. Goedert, M., Spillantini, M. G., Cairns, N. J., and Crowther, R. A. (1992) Tau proteins of Alzheimer paired helical filaments: abnormal phosphorylation of all six brain isoforms. *Neuron* **8,** 159–168
2. Grundke-Iqbal, I., Iqbal, K., Quinlan, M., Tung, Y. C., Zaidi, M. S., and Wisniewski, H. M. (1986) Microtubule-associated protein tau: a component of Alzheimer paired helical filaments. *J. Biol. Chem.* **261,** 6084–6089
3. Lee, V. M., Balin, B. J., Otvos, L. Jr., and Trojanowski, J. Q. (1991) A68: a major subunit of paired helical filaments and derivatized forms of normal Tau. *Science* **251,** 675–678
4. Horiguchi, T., Uryu, K., Giasson, B. I., Ischiropoulos, H., LightFoot, R., Bellmann, C., Richter-Landsberg, C., Lee, V. M., and Trojanowski, J. Q. (2003) Nitration of tau protein is linked to neurodegeneration in tauopathie. *Am. J. Pathol.* **163,** 1021–1031
5. Zhang, Y. J., Xu, Y. F., Chen, X. Q., Wang, X. C., and Wang, J. Z. (2005) Nitration and oligomerization of tau induced by peroxynitrite inhibit its microtubule-binding activity. *FEBS Lett.* **579,** 2421–2427
6. Radi, R., Cassina, A., Hodara, R., Quijano, C., and Castro, L. (2002) Peroxynitrite reactions and formation in mitochondria. *Free Radic. Biol. Med.* **33,** 1451–1464
7. Hensley, K., Maidt, M. L., Yu, Z., Sang, H., Markesbery, W. R., and Floyd, R. A. (1998) Electrochemical analysis of protein nitrotyrosine and dityrosine in the Alzheimer brain indicates region-specific accumulation. *J. Neurosci.* **18,** 8126–8132
8. Tohgi, H., Abe, T., Yamazaki, K., Murata, T., Ishizaki, E., and Isobe, C. (1999) Alterations of 3-nitrotyrosine concentration in the cerebrospinal fluid during aging and in patients with Alzheimer's disease. *Neurosci. Lett.* **269,** 52–54
9. Smith, M. A., Richey Harris, P. L., Sayre, L. M., Beckman, J. S., and Perry, G. (1997) Widespread peroxynitrite-mediated damage in Alzheimer's disease. *J. Neurosci.* **17,** 2653–2657
10. Castegna, A., Thongboonkerd, V., Klein, J. B., Lynn, B., Markesbery, W. R., and Butterfield, D. A. (2003) Proteomic identification of nitrated proteins in Alzheimer's disease brain. *J. Neurochem.* **85,** 1394–1401
11. Good, P. F., Werner, P., Hsu, A., Olanow, C. W., and Perl, D. P. (1996) Evidence of neuronal oxidative damage in Alzheimer's disease. *Am. J. Pathol.* **149,** 21–28
12. Koppal, T., Drake, J., Yatin, S., Jordan, B., Varadarajan, S., Bettenhausen, L., and Butterfield, D. A. (1999) Peroxynitrite-induced alterations in synaptosomal membrane proteins: in-

sight into oxidative stress in Alzheimer's disease. *J. Neurochem.* **72,** 310–317
13. Zouki, C., Zhang, S. L., Chan, J. S., and Filep, J. G. (2001) Peroxynitrite induces integrin-dependent adhesion of human neutrophils to endothelial cells via activation of the Raf-1/MEK/Erk pathway. *FASEB J.* **15,** 25–27
14. Bapat, S., Verkleij, A., and Post, J. A. (2001) Peroxynitrite activates mitogen-activated protein kinase (MAPK) via a MEK-independent pathway: a role for protein kinase C. *FEBS Lett.* **499,** 21–26
15. Zhang, P., Wang, Y., Kagen, E., and Bonner, J. (2000) Peroxynitrite targets the epidermal growth factor receptor, Raf-1, and MEK independently to activate MAPK. *J. Biol. Chem.* ***275,*** 22,479–22, 486
16. Oh-hashi, K., Maruyama, W., Yi, H., Takahashi, T., Naoi, M., and Isobe, K. (1999) Mitogen-activated protein kinase pathway mediates peroxynitrite-induced apoptosis in human dopaminergic neuroblastoma SH-SY5Y cells. *Biochem. Biophys. Res. Commun.* **263,** 504–509
17. Pesse, B., Levrand, S., Feihl, F., Waeber, B., Gavillet, B., Pacher, P., and Liaudet, L. (2005) Peroxynitrite activates ERK via Raf-1 and MEK, independently from EGF receptor and p21(Ras) in H9C2 cardiomyocytes. *J. Mol. Cell Cardiol.* **38**, 765–775
18. Go, Y. M., Patel, R. P., Maland, M. C., Park, H., Beckman, J. S., Darley-Usmar, V. M., and Jo, H. (1999) Evidence for peroxynitrite as a signaling molecule in flow-dependent activation of c-Jun NH(2)-terminal kinase. *Am. J. Physiol.* **277,** H1647–H1653
19. Oh-Hashi, K., Maruyama, W., and Isobe, K. (2001) Peroxynitrite induces GADD34, 45, and 153 via p38 MAPK in human neuroblastoma SH-SY5Y cells. *Free Radic. Biol. Med.* **30**, 213–221
20. Spear, N., Estevez, A. G., Barbeito, L., Beckman, J. S., and Johnson, G. V. (1997) Nerve growth factor protects PC12 cells against peroxynitrite-induced apoptosis via a mechanism dependent on phosphatidylinositol 3-kinase. *J. Neurochem.* **69,** 53–59
21. Hellberg, C. B., Boggs, S. E., and Lapetina, E. G. (1998) Phosphatidylinositol 3-kinase is a target for protein tyrosine nitration. *Biochem. Biophys. Res. Commun.* **252,** 313–317
22. el-Remessy, A. B., Bartoli, M., Platt, D. H., Fulton, D., and Caldwell, R. B. (2005) Oxidative stress inactivates VEGF survival signaling in retinal endothelial cells via PI 3-kinase tyrosine nitration. *J. Cell Sci.* **118,** 243–252
23. Grimes, C. A., and Jope, R. S. (2001) The multifaceted roles of glycogen synthase kinase 3β in cellular signaling. *Prog. Neurobiol.* **65,** 391–426
24. Iqbal, K., Alonso Adel, C., Chen, S., Chohan, M. O., El-Akkad, E., Gong, C. X., Khatoon, S., Li, B., Liu, F., Rahman, A., Tanimukai, H., and Grundke-Iqbal, I. (2005) Tau pathology in Alzheimer disease and other tauopathies. *Biochim. Biophys. Acta* **1739,** 198–210
25. Schildknecht, S., Bachschmid, M., and Ullrich, V. (2005) Peroxynitrite provides the peroxide tone for PGHS-2-dependent prostacyclin synthesis in vascular smooth muscle cells. *FASEB J.* **19,** 1169–1171
26. Whiteman, M., Armstrong, J. S., Cheung, N. S., Siau, J. L., Rose, P., Schantz, J. T., Jones, D. P., and Halliwell, B. (2004) Peroxynitrite mediates calcium-dependent mitochondrial dysfunction and cell death via activation of calpains. *FASEB J.* **18,** 1395–1397
27. Bao, F., and Liu, D. (2002) Peroxynitrite generated in the rat spinal cord induces neuron death and neurological deficits. *Neuroscience* **115,** 839–849
28. Muyderman, H., Nilsson, M., and Sims, N. R. (2004) Highly selective and prolonged depletion of mitochondrial glutathione in astrocytes markedly increases sensitivity to peroxynitrite. *J. Neurosci.* **24,** 8019–8028
29. Freels, J. L., Nelson, D. K., Hoyt, J. C., Habib, M., Numanami, H., Lantz, R. C., and Robbins, R. A. (2002) Enhanced activity of human IL-10 after nitration in reducing human IL-1 production by stimulated peripheral blood mononuclear cells. *J. Immunol.* **169,** 4568–4571
30. Hickman-Davis, J., Gibbs-Erwin, J., Lindsey, J. R., and Matalon, S. (1999) Surfactant protein A mediates mycoplasmacidal activity of alveolar macrophages by production of peroxynitrite. *Proc. Natl. Acad. Sci. U. S. A.* **96,** 4953–4958
31. Morris, R. (1984) Developments of a water-maze procedure for studying spatial learning in the rat. *J. Neurosci. Methods* **11,** 47–60
32. Keller, J. N., Hanni, K. B., and Markesbery, W. R. (2000) Impaired proteasome function in Alzheimer's disease. *J. Neurochem.* **75**, 436–439
33. Goldbaum, O., Oppermann, M., Handschuh, M., Dabir, D., Zhang, B., Forman, M. S., Trojanowski, J. Q., Lee, V. M., and Richter-Landsberg, C. (2003) Proteasome inhibition stabilizes tau inclusions in oligodendroglial cells that occur after treatment with okadaic acid. *J. Neurosci.* **23,** 8872–8880
34. Wang, J. Z., Wu, Q., Smith, A., Grundke-Iqbal, I., and Iqbal, K. (1998) Tau is phosphorylated by GSK-3 at several sites found in Alzheimer disease and its biological activity markedly inhibited only after it is prephosphorylated by A-kinase. *FEBS Lett.* **436,** 28–34
35. David, D. C., Layfield, R., Serpell, L., Narain, Y., Goedert, M., and Spillantini, M. G. (2002) Proteasomal degradation of tau protein. *J. Neurochem.* **83,** 176–185
36. Luth, H. J., Munch, G., and Arendt, T. (2002) Aberrant expression of NOS isoforms in Alzheimer's disease is structurally related to nitrotyrosine formation. *Brain Res.* **953,** 135–143
37. Wang, Q., Rowan, M. J., and Anwyl, R. (2004) Beta-amyloid-mediated inhibition of NMDA receptor-dependent long-term potentiation induction involves activation of microglia and stimulation of inducible nitric oxide synthase and superoxide. *J. Neurosci.* **24,** 6049–6056
38. Tran, M. H., Yamada, K., Olariu, A., Mizuno, M., Ren, X. H., and Nabeshima, T. (2001) Amyloid beta-peptide induces nitric oxide production in rat hippocampus: association with cholinergic dysfunction and amelioration by inducible nitric oxide synthase inhibitors. *FASEB J.* **15,** 1407–1409
39. Combs, C. K., Karlo, J. C., Kao, S. C., and Landreth, G. E. (2001) beta-Amyloid stimulation of microglia and monocytes results in TNFalpha-dependent expression of inducible nitric oxide synthase and neuronal apoptosis. *J. Neurosci.* **21,** 1179–1188
40. Akama, K. T., and Van Eldik, L. J. (2000) Beta-amyloid stimulation of inducible nitric-oxide synthase in astrocytes is interleukin-1beta- and tumor necrosis factor-alpha (TNFalpha)-dependent, and involves a TNFalpha receptor-associated factor- and NFkappaB-inducing kinase-dependent signaling mechanism. *J. Biol. Chem.* **275,** 7918–7924
41. McDonald, D. R., Brunden, K. R., and Landreth, G. E. (1997) Amyloid fibrils activate tyrosine kinase-dependent signaling and superoxide production in microglia. *J. Neurosci.* **17,** 2284–94
42. Possel, H., Noack, H., Keilhoff, G., and Wolf, G. (2002) Life imaging of peroxynitrite in rat microglial and astroglial cells: role of superoxide and antioxidants. *Glia* **38,** 339–350
43. van der Vliet, A., Eiserich, J. P., O'Neill, C. A., Halliwell, B., and Cross, C. E. (1995) Tyrosine modification by reactive nitrogen species: a closer look. *Arch. Biochem. Biophys.* **319,** 341–349
44. Pei, J. J, Braak, E., Braak, H., Grundke-Iqbal, I., Iqbal, K., Winblad, B., and Cowburn, R. F. (1999) Distribution of active glycogen synthase kinase 3beta (GSK-3beta) in brains staged for Alzheimer disease neurofibrillary changes. *J. Neuropathol. Exp. Neurol.* **58,** 1010–1019
45. Shiurba, R. A., Ishiguro, K., Takahashi, M., Sato, K, Spooner, E. T., Mercken, M., Yoshida, R., Wheelock, T. R., Yanagawa, H., Imahori, K., and Nixon, R. A. (1996) Immunocytochemistry of tau phosphoserine 413 and tau protein kinase I in Alzheimer pathology. *Brain Res.* **737,** 119–32
46. Cho, J. H., and Johnson, G. V. (2003) Glycogen synthase kinase 3beta phosphorylates tau at both primed and unprimed sites: differential impact on microtubule binding. *J. Biol. Chem.* **278,** 187–193
47. Tsujio, I., Tanaka, T., Kudo, T., Nishikawa, T., Shinozaki, K., Grundke-Iqbal, I., Iqbal, K., and Takeda, M. (2000) Inactivation of glycogen synthase kinase-3 by protein kinase delta: implications for regulation of tau phosphorylation. *FEBS Lett.* **469,** 111–117
48. Liu, S. J., and Wang, J. Z. (2002) Alzheimer-like tau phosphorylation induced *in vivo* by wortmannin and its attenuation by melatonin. *Acta Pharmacol. Sin.* **23,** 183–187
49. Goedert, M., Hasegawa, M., Jakes, R., Lawler, S., Cuenda, A., and Cohen, P. (1997) Phosphorylation of microtubule-associated protein tau by stress-activated protein kinases. *FEBS Lett.* **409,** 57–62
50. Reynolds, C. H., Nebreda, A. R., Gibb, G. M., Utton, M. A., and Anderson, B. H. (1997) Reactivating kinase/p38 phosphorylates τ protein *in vitro*. *J. Neurochem.* **69,** 191–198

51. Hensley, K., Floyd, R. A., Zheng, N.-Y., Nael, R., Robinson, K. A., Nguyen, X., Pye, Q. N., Stewart, C. A., Geddes, J., Markesbery, W. R., Patel, E., Johnson, G. V. W., and Bing, G. (1999) p38 kinase is activated in Alzheimer's disease brain. *J. Neurochem.* **72,** 2053–2058
52. Zhu, X., Rottkamp, C. A., Boux, H., Takeda, A., Perry, G., and Smith, M. A. (2000) Activation of p38 kinase links Tau phosphorylation, oxidative stress, and cell cycle-related events in Alzheimer disease. *J. Neuropathol. Exp. Neurol.* **59,** 880–888
53. Sun, A., Liu, M., Nguyen, X. V., and Bing, G. (2003) p38 MAP kinase is activated at early stages in Alzheimer's disease brain. *Exp. Neurol.* **183,** 394–405
54. Zhu, X., Rottkamp, C. A., Hartzler, A., Sun, Z., Takeda, A., Boux, H., Shimohama, S., Perry, G., and Smith, M. A. (2001) Activation of MKK6, an upstream activator of p38, in Alzheimer's disease. *J. Neurochem.* **79,** 311–318
55. Feijoo, C., Campbell, D. G., Jakes, R., Goedert, M., and Cuenda, A. (2005) Evidence that phosphorylation of the microtubule-associated protein Tau by SAPK4/p38delta at Thr50 promotes microtubule assembly. *J. Cell Sci.* **118,** 397–408
56. Osna, N. A., Haorah, J., Krutik, V. M., and Donohue, T. M., Jr. (2004) Peroxynitrite alters the catalytic activity of rodent liver proteasome *in vitro* and *in vivo*. *Hepatology* **40,** 574–582
57. Lam, Y. A., Pickart, C. M., Alban, A., Landon, M., Jamieson, C., Ramage, R., Mayer, R. J., and Layfield, R. (2000) Inhibition of the ubiquitin-proteasome system in Alzheimer's disease. *Proc. Natl. Acad. Sci. U. S. A.* **97,** 9902–9906
58. Lopez Salon, M., Morelli, L., Castano, E. M., Soto, E. F., and Pasquini, J. M. (2000) Defective ubiquitination of cerebral proteins in Alzheimer's disease. *J. Neurosci. Res.* **62,** 302–310
59. Reynolds, M. R., Berry, R. W., and Binder, L. I. (2005) Site-specific nitration and oxidative dityrosine bridging of the tau protein by peroxynitrite: implications for Alzheimer's disease. *Biochemistry* **44,** 1690–1700
60. Hodara, R., Norris, E. H., Giasson, B. I., Mishizen-Eberz, A. J., Lynch, D. R., Lee, V. M., and Ischiropoulos, H. (2004) Functional consequences of alpha-synuclein tyrosine nitration: diminished binding to lipid vesicles and increased fibril formation. *J. Biol. Chem.* **279,** 47,746–47, 753
61. Lee, V. M., Giasson, B. I., and Trojanowski, J. Q. (2004) More than just two peas in a pod: common amyloidogenic properties of tau and alpha-synuclein in neurodegenerative diseases. *Trends Neurosci.* **27,** 129–134
62. Hyun, D. H., Lee, M., Halliwell, B., and Jenner, P. (2003) Proteasomal inhibition causes the formation of protein aggregates containing a wide range of proteins, including nitrated proteins. *J. Neurochem.* **86,** 363–373
63. Liu, S. J., Zhang, J. Y., Li, H. L., Fang, Z. Y., Wang, Q., Deng, H. M., Gong, C. X., Grundke-Iqbal, I., Iqbal, K., and Wang, J. Z. (2004) Tau becomes a more favorable substrate for GSK-3 when it is prephosphorylated by PKA in rat brain. *J. Biol. Chem.* **279,** 50078–50088
64. Cardozo, C., and Michaud, C. (2002) Proteasome-mediated degradation of tau proteins occurs independently of the chymotrypsin-like activity by a nonprocessive pathway. *Arch. Biochem. Biophys.* **408,** 103–110
65. Hooper, D. C., Scott, G. S., Zborek, A., Mikheeva, T., Kean, R. B., Koprowski, H., and Spitsin, S. V. (2000) Uric acid, a peroxynitrite scavenger, inhibits CNS inflammation, blood-CNS barrier permeability changes, and tissue damage in a mouse model of multiple sclerosis. *FASEB J.* **14,** 691–698
66. Hooper, D. C., Spitsin, S., Kean, R. B., Champion, J. M., Dickson, G. M., Chaudhry, I., and Koprowski, H. (1998) Uric acid, a natural scavenger of peroxynitrite, in experimental allergic encephalomyelitis and multiple sclerosis. *Proc. Natl. Acad. Sci. U. S. A.* **95,** 675–680
67. Scott, G. S., Cuzzocrea, S., Genovese, T., Koprowski, H., and Hooper, D. C. (2005) Uric acid protects against secondary damage after spinal cord injury. *Proc. Natl. Acad. Sci. U. S. A.* **102,** 3483–3488
68. El-Remessy, A. B., Behzadian, M. A., Abou-Mohamed, G., Franklin, T., Caldwell, R. W., and Caldwell, R. B. (2003) Experimental diabetes causes breakdown of the blood-retina barrier by a mechanism involving tyrosine nitration and increases in expression of vascular endothelial growth factor and urokinase plasminogen activator receptor. *Am. J. Pathol.* **162,** 1995–2004
69. Lee, V. M., Goedert, M., and Trojanowski, J. Q. (2001) Neurodegenerative tauopathies. *Annu. Rev. Neurosci.* **24,** 1121–1159
70. Johansson, A. C., Steen, H., Ollinger, K., and Roberg, K. (2003) Cathepsin D mediates cytochrome *c* release and caspase activation in human fibroblast apoptosis induced by staurosporine. *Cell Death. Differ.* **10,** 1253–1259
71. Lee, H. G., Perry, G., Moreira, P. I., Garrett, M. R., Liu, Q., Zhu, X., Takeda, A., Nunomura, A., and Smith, M. A. (2005) Tau phosphorylation in Alzheimer's disease: pathogen or protector? *Trends Mol. Med.* **11,** 164–169
72. Morsch, R., Simon, W., and Coleman, P. D. (1999) Neurons may live for decades with neurofibrillary tangles. *J. Neuropathol. Exp. Neurol.* **58,** 188–197
73. Shringarpure, R., Grune, T., and Davies, K. J. (2001) Protein oxidation and 20S proteasome-dependent proteolysis in mammalian cells. *Cell Mol. Life Sci.* **58,** 1442–1450
74. Coux, O., Tanaka, K., and Goldberg, A. L. (1996) Structure and functions of the 20S and 26S proteasomes. *Annu. Rev. Biochem.* **65,** 801–847

Received for publication October 4, 2005.
Accepted for publication January 4, 2006.